

# A Model of Saccade Initiation Based on the Competitive Integration of Exogenous and Endogenous Signals in the Superior Colliculus

Thomas P. Trappenberg<sup>1</sup>, Michael C. Dorris<sup>2</sup>, Douglas P. Munoz<sup>2</sup>, and Raymond M. Klein<sup>3</sup>

## Abstract

■ Significant advances in cognitive neuroscience can be achieved by combining techniques used to measure behavior and brain activity with neural modeling. Here we apply this approach to the initiation of rapid eye movements (saccades), which are used to redirect the visual axis to targets of interest. It is well known that the superior colliculus (SC) in the midbrain plays a major role in generating saccadic eye movements, and physiological studies have provided important knowledge of the activity pattern of neurons in this structure. Based on the observation that the SC receives localized sensory (exogenous) and voluntary (endogenous) inputs, our model assumes that this information is integrated

by dynamic competition across local collicular interactions. The model accounts well for the effects upon saccadic reaction time (SRT) due to removal of fixation, the presence of distractors, execution of pro- versus antisaccades, and variation in target probability, and suggests a possible mechanism for the generation of express saccades. In each of these cases, the activity patterns of “neurons” within the model closely resemble actual cell behavior in the intermediate layer of the SC. The interaction structure we employ is instrumental for producing a physiologically faithful model and results in new insights and hypotheses regarding the neural mechanisms underlying saccade initiation. ■

## INTRODUCTION

An established principle in neuroscience is the distributed nature of brain processes. One consequence of multiple processing streams (e.g., Milner & Goodale, 1995; Ungerleider & Mishkin, 1982) is that to produce appropriate behavioral responses, there must be mechanisms of information integration. A well-studied example of this principle is that of saccadic eye movements. At any moment in time, there is only one location to which we can direct our foveae despite the fact that many potential targets may be present. Selecting the target for a saccade entails the integration of multiple sources of information. One proposed location for the integration of signals from several information processing pathways in the brain is the intermediate layers of the superior colliculus (SC), a midbrain neural structure receiving convergent afferents from a multitude of cortical and subcortical visual and cognitive centers related to eye movement control (see Sparks & Hartwich-Young, 1989 for a review). The SC, in turn, sends extensive projections to the brainstem premotor circuitry to trigger saccadic eye movements (Moschova-

kis, 1996). The SC therefore functions as a crucial integrative structure between higher cortical processing centers and the brainstem premotor circuit. In this article, we develop and describe a simple neural field model of this integration mechanism. We show that the dynamic properties of this model can account for many observations related to the timing of the initiation of saccadic eye movements in primates and that the behavior of this model’s artificial neurons (nodes) closely reflects the activity patterns of real neurons in the intermediate layers of the SC.

Kopecz (1995) (see also Kopecz & Schöner, 1995) demonstrated that some saccadic reaction time (SRT) behaviors can be modeled by a mechanism where two kinds of signal, visual (exogenous) and instructional (endogenous), converge within a dynamical integration layer employing lateral interactions characterized by short-distance excitation and long-distance inhibition. In this article, we take this idea further in several important ways. First, we report on our physiological evidence demonstrating that such a dynamic mechanism could indeed be realized in the SC. Second, we advance the hypothesis that the mechanism outlined by Kopecz and Schöner is located in the intermediate layers of the SC and we compare the performance of the model both with behavioral data in humans and monkeys and with

---

<sup>1</sup> University of Oxford, UK, <sup>2</sup> Queen’s University, Canada, <sup>3</sup> Dalhousie University, Canada

recordings of SC cell activities in monkeys. Third, we make successive modifications to the model to more closely reflect the activity patterns of cells in the intermediate layer of the SC while maintaining a reasonable fit to the performance data (SRTs). Finally, we demonstrate the robustness of our model by its ability to simulate behavior and cell patterns when the system is subjected to a variety of well-studied oculomotor tasks while changing only task-related parameters of the model.

As mentioned above, the SC is known to be a critical structure for massive convergence of inputs from a multitude of cortical and subcortical areas involved in sensory, motor, and attentional processing. In order to simplify the model, we classify inputs to the SC into two broad, conceptually defined classes using the terms “exogenous” to refer to only marginally processed sensory inputs (corresponding to Kopecz and Schöner’s visual input), and “endogenous” (corresponding to Kopecz and Schöner’s instructional input) to refer to voluntary inputs, which are dependent on task-related instructions or expectancies (Klein, Kingstone, & Pontefract, 1992; Posner, 1980). Although exogenous and endogenous signals can have their origin in sensory inputs from various modalities, in this article, we concentrate mainly on visual signals. Before introducing some of the key attributes of the model, we will first discuss the manipulations against which it will be tested.

### **Gap Effect**

A global reduction in SRTs to all target locations occurs with removal of a centrally foveated fixation point prior to the presentation of a peripheral target compared to the condition in which the fixation point is not removed (Reuter-Lorenz, Hughes, & Fendrich, 1991). This reduction in SRT, associated with the introduction of a “gap” period between fixation point disappearance and target appearance, was first characterized by Saslow (1967) and has been termed the gap effect. It has been demonstrated that the gap effect has both an exogenous and an endogenous component. Removal of the fixation point results in an automatic (exogenous) fixation disengagement, which is associated with changes in the discharge rates of fixation-related neurons in the SC (Dorris & Munoz, 1995; Dorris, Paré, & Munoz, 1997). In addition, the removal of the fixation point acts as a timing or warning signal that allows the subject to prepare to make a saccade by endogenously disengaging from fixation in advance of the impending target. This endogenously driven warning effect can be replicated by maintaining the fixation point throughout a trial while presenting an auditory warning signal just prior to target presentation (Taylor, Kingstone, & Klein, 1998; Reuter-Lorenz et al., 1991; Ross & Ross, 1981).

### **Distractors**

Experiments with distractors provide useful data for exploring the effects of competing visual exogenous inputs. In these experiments, two visual signals are presented, one of which is defined—by instruction—as task-relevant (target), the other of which is defined as task-irrelevant (distractor) and is therefore presumed not to generate an endogenous component. Distractors presented simultaneously far or near from a saccadic target increase or decrease SRTs, respectively (Walker, Deubel, Schneider, & Findlay, 1997; Corneil & Munoz, 1996). This paradigm can also be used to study effective collicular interactions that are critical for quantifying the structure of our model (Olivier, Dorris, & Munoz, 1999). We have estimated this interaction by recording cellular activity in the SC of nonhuman primates during a distractor experiment wherein irrelevant stimuli are presented shortly before target onset. Recordings of cellular activity reveal a direct influence of distractors, which we assume to be purely exogenous, upon neuronal prelude activity in advance of target-directed saccades, which we assume have an endogenous component.

### **Pro- Versus Antisaccades**

By comparing the typical prosaccade task (look at a target) with an “antisaccade” task, in which one stimulus is presented but the correct response is to look in the opposite direction, one can explore the consequence of placing exogenously and endogenously activated saccadic programs in direct conflict with one another. To perform the “antisaccade” task correctly, incorrect reflexive prosaccades must be inhibited and extra time must be taken to generate the proper metrics of the antisaccade (see Everling & Fischer, 1998 for a review). Consistent with human performance data, our model produces antisaccades with longer latencies than prosaccades.

### **Target Expectancies**

We discuss experiments in which endogenous signals related to expectations are varied systematically by presenting saccadic targets at locations with varied probability of target appearance (Basso & Wurtz, 1998; Dorris & Munoz, 1998; Simpson & Klein, 1997; Trappenberg et al., 1997; Carpenter & Williams, 1995; Klein & Pontefract, 1994). We demonstrate that our model is able to reproduce not only the behavioral pattern of humans (Simpson & Klein, 1997) and monkeys (Dorris & Munoz, 1998), but also the activity profiles of neurons in the SC reflecting endogenous signals (Dorris & Munoz, 1998).

### **Express Saccades**

When an exogenous target is coupled with endogenously generated saccadic preparation (i.e., high prob-

ability or training to specific target location) and exogenously generated disengagement from fixation (due to removal of the fixation stimulus), the result can be an extremely fast mode of SRTs known as express saccades (see for reviews Paré & Munoz, 1996; Fischer & Weber, 1993). We discuss and demonstrate how such extremely fast SRTs and a bimodal distribution of SRTs are produced within the framework of our model.

## THE MODEL

Our model is purposely kept on a level of description intended to stress how the simple mechanism of “dynamic-integration-by-competition” influences SRTs. Similar models with competitive interaction, often termed simply “neural field models,” have been proposed for other brain areas (see, e.g., Jancke et al., 1999; Samsonowich & McNaughton, 1997; Taylor & Alavi, 1995, 1997; Usher, Stemmler, Koch, & Olami, 1996), suggesting that this class of model may be capturing a fundamental mechanism of brain information processing (Desimone & Duncan, 1995). However, it is important to note that the details in our model are designed specifically to account for how the neuronal activity within the intermediate layers of the SC can produce saccadic behavior in a range of situations involving the interaction of endogenous and exogenous signals.

### Model Architecture and Dynamics

Saccade-related neurons in the intermediate layers of the SC can be classified on the basis of discharge characteristics in oculomotor tasks. For example, Munoz and Wurtz (1993, 1995a) classified these neurons into fixation, buildup, and burst neurons. Fixation neurons, located at the rostral pole of each colliculus, display tonic activity during periods of fixation and have a pause in their discharge associated with saccades (Munoz & Wurtz, 1993). The majority of both burst and buildup neurons, located more caudally in the SC, have a high frequency burst of activity associated with the presentation of visual stimuli and generation of saccades into their response fields (Munoz & Wurtz, 1995a). Buildup neurons, in addition, have low frequency activity that begins during the delay period of many oculomotor tasks, such as the gap paradigm, which is reciprocal to the decrease in activity in fixation neurons during this same period (Dorris & Munoz, 1995; Dorris et al., 1997; Munoz & Wurtz, 1995a). These three classes of neurons, in turn, project to the brainstem reticular formation (Istvan, Dorris, & Munoz, 1994) where the final stage of the saccade-generating circuitry is located (Moschovakis, 1996).

The structure of our model of the intermediate layer of the SC is outlined in Figure 1A. The central nodes represent fixation neurons (green) in the rostral pole of

the SC, whereas peripheral nodes represent buildup neurons (blue) and burst neurons (red) of the left and right colliculus, respectively. It should be noted that fixation nodes are essentially buildup nodes with foveal as opposed to peripheral receptive fields. We use this one-dimensional structure to generate the simulations illustrated in this article. It has been shown that the important characteristics of such a one-dimensional model (Amari, 1977) generalize to higher dimensions (Taylor, 1999; Konen, Maurer, von der Malsburg, 1994). Neurons in the SC are modeled as simple nodes. The time dependent internal state of the nodes is denoted by  $u_i(t)$  and is intended to simulate the average membrane potential of the neurons. The activity  $A(t)$  of a node is given as a nonlinear function of its internal state using a common sigmoidal function:

$$A_i(t) = \frac{1}{1 + \exp(-\beta u_i(t) + \theta)} \quad (1)$$

with parameters  $\beta$  and  $\theta$  defining the steepness and the offset of the sigmoid, respectively. When comparing the model’s behavior to that of the biological system it represents, the activation level of a node is interpreted as an average firing rate. Whereas our model is, thus, expressly at the level of average firing rates, it is important to note that the effects we describe would be expected in corresponding models with spiking neurons (Trappenberg, 1998a, 1998b).

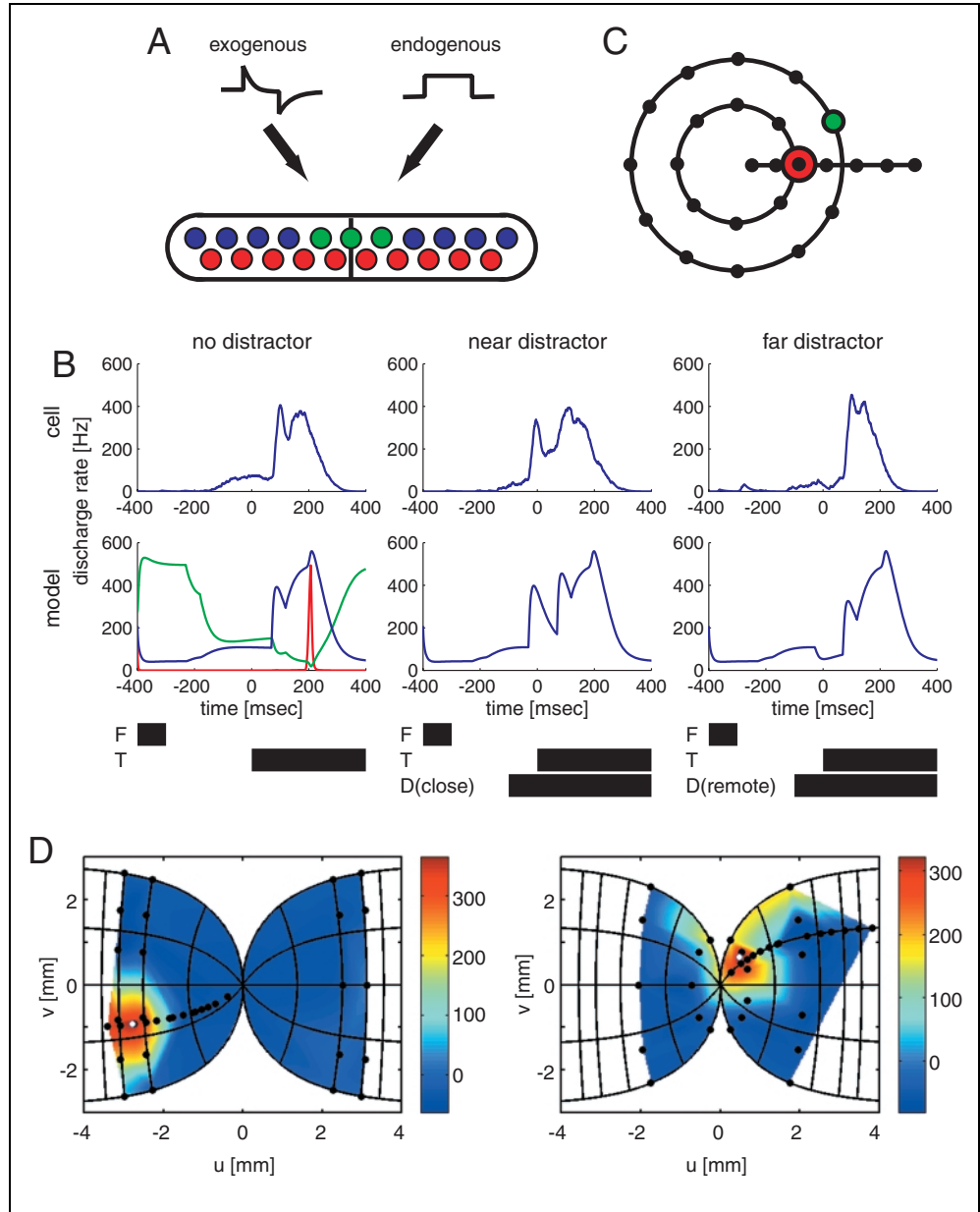
The dynamics of the internal state  $u_i(t)$  of a node with index  $i$  (which corresponds to its spatial location within the map) can be described by the following differential equation:

$$\tau \frac{du_i(t)}{dt} = -u_i(t) + \sum_j w_{ij} A_j(t) + I_i^{\text{in}}(t) - u_0 + a_\eta \eta(t) \quad (2)$$

where  $\tau$  is a time constant,  $w_{ij}$  is the synaptic efficacy (weight) from node  $i$  to node  $j$ ,  $A_j$  is the activity of node  $j$ , and  $I_i^{\text{in}}$  describes the input from other noncollicular areas (such as cortical and subcortical inputs) into this cell assembly. The value of the global constant  $u_0$  is the only difference between burst nodes and buildup/fixation nodes. This constant is set to zero for buildup nodes, whereas the burst nodes receive a strong global inhibition during active fixation, which ceases only after the discharge of buildup nodes reach a certain threshold (see section on the choice of parameters for more details).

The last term,  $\eta(t)$ , is a random variable introduced to simulate fluctuations in the oculomotor circuitry (Dorris, Paré, & Munoz, 2000; Ratcliff, Van Zandt, & McKoon, 1999). Here, we use a normally distributed random variable,  $\eta = N(0,1)$ , and adjust the strength by a factor  $a_\eta$ . This term was used to verify that the findings are stable under conditions resembling the fluctuations in the waveforms derived from the cell recordings. How-

**Figure 1.** (A) Model architecture reflecting the intermediate layer of the SC with fixation cells (green), buildup cells (blue), and burst cells (red). The inputs to this layer are classified as exogenous and endogenous. Their respective time course is shown schematically corresponding to an onset and offset. Both inputs have a Gaussian spatial distribution not shown in the figure. (B) Discharge pattern of buildup cells in the distractor experiments. Upper row: cell recording data. Second row: model simulations. The corresponding presentations of the fixation (F), target (T), and distractor (D) are shown at the bottom. In the left column, no distractor was presented, whereas the remaining graphs show results with a distractor in near (middle column) and remote (right column) proximity to the target. (C) Schematic outline of distractor locations in visual space. The distractor locations in each experiment, when converted to anatomical positions within the SC, are shown as black points in (D). (D) Two examples of the influence of the distractor on the buildup activity of buildup cells in the intermediate layer of the SC. White point: estimated preferred direction of the recorded cell from the maximal enhancement of buildup activity by a distractor. Black point: estimated center of the receptive field corresponding to the distractor location. The color scheme represents the distractor-related enhancement (reduction in dark blue) in buildup activity in spikes/sec.



ever, most of the simulations do not require this noise and it is therefore omitted to display more clearly the average behavior of the system. In this article, the noise term is only used to simulate SRT distributions when discussing express saccades (see section on Express Saccades).

### Converging Exogenous and Endogenous Inputs

Factors influencing saccade initiation can be broadly categorized into exogenous and endogenous domains (Klein & Shore, 2000; Forbes & Klein, 1996; Kopecz, 1995). Our model SC layer therefore receives two

types of input: exogenous (exo) and endogenous (endo),

$$I^{in} = I^{exo} + I^{endo} \quad (3)$$

where both types of input have a Gaussian spatial shape, so that the input at location  $k$  is given by:

$$\tilde{I}_i^{exo,endo}(k) = a_{exo,endo} \exp\left(-\frac{(k-l)^2}{2\sigma_{in}^2}\right) \quad (4)$$

when the signal is centered at location  $l$ . The width of the Gaussian was derived from the shape of movement fields of saccade-related neurons in the monkey SC (Munoz & Wurtz, 1995b). However, the precise spatial

form of the input is not critical for the findings in this article, because information is also spreading laterally within the SC through the effective pathways therein (see below).

The position and the time of onset (and offset) of events leading to inputs to the model depend upon experimental conditions. The exogenous input derives from sensory information reaching the SC without extensive information processing and is hence taken to follow closely the onset of a visual stimulus in the periphery with a delay ( $t_{\text{delay}}^{\text{exo}}$ ). In contrast, endogenous input requires interpretation by higher processing centers to determine the behavioral response that would be appropriate for the given task instructions. For example, in the simultaneous distractor paradigm (Figure 3B, 0 msec condition), exogenous inputs associated with the target and distractor are equivalent except for location (they activate different regions of the one-dimensional field). The endogenous input is delivered only to the region representing the correct response (target). The longer time ( $t_{\text{delay}}^{\text{endo}} > t_{\text{delay}}^{\text{exo}}$ ) for endogenous input due to additional, presumably cortical, processing.

From the point of view of the model, these two types of input differ not only in their latency, but also in their temporal dynamics (time-course). Although there is little direct evidence on the time-course of exogenous inputs to the SC, cell recordings do reveal a transient component closely following the appearance or disappearance of an external stimulus, which we identify with the exogenous signal. We therefore model the time-course of exogenous inputs as:

$$\tau_{\text{on,off}} \frac{dI_i^{\text{exo}}(t)}{dt} = -I_i^{\text{exo}} + \tilde{I}^{\text{exo}} \delta(t - t_{\text{on,off}} - t_{\text{delay}}^{\text{exo}}) \quad (5)$$

where we included a transient offset component as suggested by Kopecz (1995) to conform with behavioral data.

Even less can be said about the time-course of endogenous signals. Hence, we also follow Kopecz (1995) by making the simplest choice of a signal, which is simply switched on and off at the appropriate time:

$$I_i^{\text{endo}}(t) = \begin{cases} \tilde{I}^{\text{endo}} & \text{if } t_{\text{on}} + t_{\text{delay}}^{\text{endo}} \leq t \leq t_{\text{off}} + t_{\text{delay}}^{\text{endo}} \\ 0 & \text{else} \end{cases} \quad (6)$$

The onset and offset of endogenous signals in the brain are likely to be more gradual. However, the simple form of Equation 6 is sufficient for our purposes in this article.

### The Lateral Interaction Structure

The critical feature of our model, which will be central to the explanation of the sensitivity of SRTs to various

experimental manipulations, is the effective interaction structure within the SC layer. Both anatomical (Olivier, Porter, & May, 1998; Behan & Kime, 1996; Mize, Jeon, Hamada, & Spencer, 1991) and physiological (Meredith & Ramoa 1998; Munoz & Istvan, 1998; McIlwain, 1982) studies have found evidence for lateral interactions within the SC. Particularly pertinent is evidence for short-distance excitation within the SC including inter-collicular excitatory connections between fixation neurons in the opposite SC and for long-distance inhibitory connections within each colliculus and between colliculi.

The essence of these studies is captured by the choice of the interaction matrix  $w$  that depends only on the spatial distance between nodes and is positive (excitatory) for short distances and negative (inhibitory) between nodes far apart from each other. From our measurements, described below, we found that the following parameterization is adequate to describe the interaction structure within the SC:

$$w_{ij} = a \exp\left(\frac{-(j-i)^2}{2\sigma_a^2}\right) - b \exp\left(\frac{-(j-i)^2}{2\sigma_b^2}\right) - c \quad (7)$$

We do not consider any learning effects, and will therefore keep the interaction (weight) matrix  $w$  constant throughout the simulations. A similar form of interaction was assumed by Kopecz (1995) and Kopecz and Schöner (1995), and was most notably found by Arai, Keller, and Edelman (1994) after training a recurrent network using spatio-temporal data from cell recordings of the SC in monkeys. It should be noted that this effective interaction pattern need not result from neural mechanisms within the SC alone. This form of  $w$  could, for example, result from a combination of short-range excitatory SC neurons and a target-sensitive inhibition from other brain areas. A prime candidate for extra-collicular inhibition would be projections from the substantia nigra pars reticulata of the basal ganglia (see Hikosaka, 1989 for a review).

Amari (1977) has studied models with a similar interaction structure and demonstrated that several different classes of asymptotic behavior emerge from the internal connections in such structures when external input is removed. First, in the case of a strong mutual excitation of each cell resulting from the lateral interactions and the global constant  $u_0$ , there will be a global buildup of activity with potentials growing without bound. Certainly, this region of the parameter space is not desirable in our model. Second, in the case of a strong mutual inhibition, the activity will globally decay resulting in an asymptotic inactive neuronal assembly. Third, there is a parameter region (characterized by neither strong mutual inhibition nor excitation), where large localized areas of active cells are stable. Kopecz (1995) and Kopecz and Schöner (1995) argued that this region is of particular interest

for describing saccadic eye movements. However, these classes describe the asymptotic behavior of the model without external input. In our simulations, we always assume some input (at least endogenous), and under this assumption, the distinction between the last two classes becomes less critical. Indeed, our model operates mostly in the second domain, which is another minor departure from the simulations by Kopecz and Schöner.

### Choice of Parameters

There are a variety of parameters in the model that are not given a priori and for which appropriate values must be chosen for the numerical simulations. Our choice was thereby guided by experimental measurements or by selecting reasonable values when direct experimental measurements were not available. The values used throughout this article should be seen as examples for which the model exhibits dynamic effects closely resembling the observed cellular and behavioral findings. Our findings are nevertheless stable in the sense that we achieved similar results when the variables are changed within a reasonable range.

Our goal is to outline the mechanism leading to the typical pattern of variability of SRTs in several paradigms in primates. A further goal was to verify that various findings in behavioral and physiological studies can be reproduced consistently within the same model. We therefore kept the system parameters constant between the simulations of the various paradigms, and altered only the parameters associated with the signals (amplitude and timing), which are plausibly paradigm-dependent. It is important to note that we were primarily interested in a qualitative fit, and did not attempt to fine-tune the parameters to match exactly the SRTs reported in human and monkey studies. The parameters might also vary within individuals and are presumably different between humans and monkeys. However, the general trend of SRTs in the paradigms explored remains consistent throughout. The parameters of our model, and the specific values used in the simulations described in this article, are briefly rationalized below.

*Architectural Parameters:*  $N = 1001$ ,  $\Delta t = 1 \text{ msec}$

All simulations reported in this article were done with  $N = 1001$  nodes, 501 buildup nodes and 500 burst nodes, reflecting 5 mm of each colliculus. This number of nodes is sufficient to capture the continuous spatial behavior of the model. The integration step was usually set to 1 msec, which provides a temporal grain sufficient to approximate the continuous dynamics reasonably well. Simulations were also verified with considerably smaller as well as larger time steps and with different numbers of nodes.

*Input Parameters:*  $\sigma_{in} = 0.7 \text{ mm}$ ,  $t_{delay}^{exo} = 70 \text{ msec}$ ,  $t_{delay}^{endo} = 120 \text{ msec}$ ,  $\tau_{on} = 10 \text{ msec}$ ,  $\tau_{off} = 70 \text{ msec}$

The width of input stimuli reaching the nodes was taken to be consistent with the average width of the movement fields of saccade-related neurons and population activity in the intermediate layers of the SC (Munoz & Wurtz, 1995b). The afferent delays,  $t_{delay}$ , of exogenous and endogenous inputs were chosen so that the simulations resemble the cell data of the macaque monkeys in this study. The latency of visual responses of neurons in the intermediate layers of the SC in monkeys studied in the Munoz laboratory is always greater than 50 msec and usually about 70 msec (Dorris et al., 1997); the typical time for the delay of endogenous input is assumed to be about 120 msec.

### Output Parameters

SRTs were calculated from the time burst cells reach 80% of their maximal discharge rate. An additional 20 msec efferent delay was added, which is a typical value found in recording and stimulation studies (Munoz & Wurtz, 1995a; Sparks, 1978; Robinson, 1972).

*SC Dynamics:*  $\tau = 10 \text{ msec}$ ,  $u_0 = 0$  or  $u_0 = 100$

The activity of buildup neurons increases during the gap or instructed delay periods in saccadic tasks (e.g., Dorris et al., 1997; Dorris & Munoz, 1998; Munoz & Wurtz, 1995a). The global inhibition was therefore set to  $u_0 = 0$  for these model cells. Burst neurons remain silent during these periods and we therefore employed a strong inhibition of  $u_0 = 100$  at the beginning of the simulation. This inhibition is removed instantaneously when the buildup nodes reach 80% of their maximal discharge rate. The initial configuration is restored by the time the burst nodes reach 80% of their maximal discharge rate at which time the endogenous signal is also restored to the initial fixation condition.

*Node Parameters:*  $\beta = 0.07$ ,  $\theta = 0$

An increasing value of  $\beta$  turns the output characteristic of a node more towards the binary mode (on/off). As buildup nodes show much variation of firing rates in a medium range, we chose this parameter to be rather small. The shift of the sigmoid function was arbitrarily set to zero.

*Interaction Matrix:*  $a = 144$ ,  $b = 48$ ,  $c = 16$ ,  $\sigma_a = 0.6 \text{ mm}$ ,  $\sigma_b = 3\sigma_a$

Special attention has been given to the determination of the interaction matrix. The distractor experiments discussed below revealed a general shape of the interaction profile resembling the form of a Mexican hat similar to that proposed by others (Kopecz, 1995; Arai et al.,

1994). The particular values of the parameters above have been chosen to fit the experimental data with the simulations.

*Input Parameters (Paradigm-Dependent):*  $t^{\text{on}}$ ,  $t^{\text{off}}$ ,  $a_{\text{exo}}$ ,  $a_{\text{endo}}$

The only parameters which have been varied between different paradigms are the onset and offset times,  $t^{\text{on}}$  and  $t^{\text{off}}$ , of exogenous and endogenous input signals, as well as their associated strength values,  $a_{\text{exo}}$  and  $a_{\text{endo}}$ . The values used will be described throughout the text. Typical values of the strength, which are only modulated slightly, are:  $a_{\text{endo}} = 10$  during active fixation (at the beginning of the run) and the restoration of fixation (at the end of the run), and  $a_{\text{exo}} = 3$  during a gap interval. The amplitude of exogenous signals were in the range of  $a_{\text{exo}} = 50$  to 70. The strength of the fixation offset was usually set to  $a_{\text{exo}} = -10$ .

## SIMULATIONS

### Buildup Activity and the Gap Effect

The characteristic increase in the discharge of buildup neurons following fixation removal in the gap paradigm (Dorris et al., 1997; Dorris & Munoz, 1998; Munoz & Wurtz, 1995a) is illustrated in the upper left panel of Figure 1B. In this experiment, monkeys are required to fixate on the center of a screen initially marked with a fixation point (FP). After the FP is removed, the screen remains dark for a period of time (gap interval = 300 msec) until a target (T) is presented in the response field of the neuron, and the monkey is required to make a saccade to the target. The buildup activity, beginning during the gap period, is followed by a transient visual burst after target appearance and a second motor burst initiating the saccade to the target.

The pattern of activation of buildup nodes in our model, which closely reflects this basic cell behavior, is displayed as a blue line in the lower left graph of Figure 1B. The model was started with an initial value of  $u_i(t = -400) = -10$  for the membrane potential of each node. The times of fixation point disappearance and target appearance were the same as in the monkey experiment and are shown schematically at the bottom of Figure 1B. In these simulations, the visual input amplitude was set to  $a_{\text{exo}} = 60$ , and the endogenous amplitude at fixation was reduced from  $a_{\text{endo}} = 10$  to  $a_{\text{endo}} = 3$  during the gap period. In addition, we show the simultaneous average firing rate of a node in the rostral pole (fixation node) with a green line in Figure 1B (lower left panel). The reciprocal behavior of buildup and fixation nodes is analogous to the behavior of such neurons in monkeys (Dorris et al., 1997; Munoz & Wurtz, 1995a). The decay of the fixation activity, therefore, has two components which can be distinguished in

the model simulations: an exogenous component, directly related to the visual fixation offset; and an endogenous component (Taylor et al., 1998), related to preparation imparted by any signal that provides a reliable warning (which in this case is also the disappearance of the fixation point).

Finally, the red line in Figure 1B (lower left panel) corresponds to the discharge profile of a burst node. The saccade is generated during activation of the burst nodes. The simulated burst discharge for burst nodes is extremely brief, resulting from our simplified implementation with instant removal of inhibition to the burst nodes once buildup activity reaches 80% of its peak value, and instant reestablishment of inhibition after the burst activity reaches 80% of its peak. Burst node activity would assume a more realistic shape if inhibition were applied and removed more gradually. Also, we used a strong inhibition of the burst layer during active fixation so that these nodes did not respond to exogenous input as seen sometimes in cell recording data (Dorris et al., 1997; Munoz & Wurtz, 1995a). We have not implemented more details at this stage, as the effects under discussion do not critically depend on these characteristics. We keep the model as simple as possible without introducing too many parameters and concentrate instead on the dynamic of buildup nodes.

### Distractors

#### *The Effective Interaction Profile Within the SC*

It is well established that neurons in the intermediate layers of the SC are organized into a topographical map for saccade generation (Van Gisbergen, Van Opstal, & Tax, 1987; Robinson 1972). Direct electrical stimulation of a particular area in this map will initiate a saccade with corresponding direction and amplitude into the contralateral visual field. In addition, many neurons in the intermediate layer of the SC also display transient discharge following visual stimuli. The locations of the visual receptive fields of these neurons overlap the movement fields (Schiller & Wurtz, 1975). Therefore, visual cues can be used to excite specific populations of neurons in the SC that drive saccades to those visual stimuli.

We explored the interaction structure in the SC by employing a distractor paradigm (Olivier et al., 1998, 1999) while recording visual responses from neurons in the intermediate layers of the SC. In these experiments, a visual stimulus (distractor) was presented during the gap interval of 100 msec before target appearance. This irrelevant distractor was distinguished by color from the target, and subjects were instructed to ignore it. This irrelevant stimulus can, nevertheless, influence SRTs in various ways. For example, if it is presented spatially near the target, shorter SRTs are observed (Olivier et al., 1999; Walker et al., 1997; Corneil & Munoz, 1996); in

contrast, longer SRTs are observed when the stimulus is presented remote from the target location. In this article, we refer to such nontarget stimuli as “distractors,” regardless of their spatial relation to the target.

The average discharge pattern of the previously described buildup neuron is shown in the upper middle panel in Figure 1B from trials where a visual distractor was presented near the target. Compared to trials without distractors (Figure 1B, upper left panel), an additional peak of discharge occurred 70 msec after the presentation of the distractor, which is a visual response related to the sudden appearance of the visual distractor in the neuron’s response field. The response of the same buildup neuron from trials where a visual distractor was presented remote from the cell’s response field is shown in the upper right panel of Figure 1B. Instead of an increase in discharge, as was the case with a near distractor, the remote distractor led to inhibition of the buildup activity (upper right panel). This attenuation of buildup activity induced by the remote distractor is a clear indication of effective long-distance inhibition realized at the level of the SC.

The influence of near and remote distractors on buildup activity (measured in relation to buildup activity in a no distractor baseline condition) can be used to map the effective interaction structure within the SC. To do this, we performed experiments where visual distractors were presented at various locations relative to the preferred vector (direction and amplitude) of the recorded cell. A schematic outline of the relative locations of the distractors in the visual field is shown in Figure 1C. The monkey was required to generate a saccade to a red target that was always presented in the center of a neuron’s response field 300 msec after fixation point disappearance in a block of trials. The center of the response field of the neuron is shown as the red area in Figure 1C. On the majority of trials, a green distractor was presented 100 msec before target presentation at some location in the visual field indicated by the black points in Figure 1C. On a small proportion of trials, no distractor (control condition) was presented.

In the analysis of the cell data, we converted the visual location of the distractors and the preferred location of the cell to anatomical locations within the SC with the following transformation formulas (Van Gisbergen et al., 1987):

$$u = B_u \ln \left( \frac{\sqrt{R^2 + 2AR \cos(\Phi)}}{A} \right) \quad (8)$$

$$v = B_v \operatorname{atan} \left( \frac{R \sin(\Phi)}{R \sin(\Phi) + A} \right) \quad (9)$$

In these formulae,  $u$  represents the anatomical distance (in mm) from the rostral pole in the SC along the axis representing horizontal position,  $v$  is the perpendicular

distance, and  $R$  and  $\Phi$  are the retinal eccentricity and the meridional direction, respectively, of the target (in degrees). The remaining symbols represent constants with the following values:  $B_u = 1.4$  mm;  $B_v = 1.8$  mm/rad; and  $A = 3^\circ$ . The calculated anatomical locations corresponding to the visual locations of the distractor are shown as black dots in Figure 1D, whereas the estimated preferred location of the cell is shown as white dot in Figure 1D.

We define an interaction indicator as the value of the discharge rate at the maximum (or minimum) of the distractor-related peak (or dip) relative to the buildup activity in the control condition in which no distractor was presented. Results of this analysis are summarized in Figure 1D for two sample buildup neurons.<sup>1</sup> The black points indicate distractor locations where this interaction indicator was sampled and areas between the points were interpolated with a cubic fit. This analysis indicates that the effect of the distractor depended mainly on the distance between the distractor location and the preferred vector of the neuron. Furthermore, the comparison of the pattern of the two cells suggests that this interaction profile is roughly independent of the location of the cell within the SC. This finding allows us to collapse the data from these two cells into one graph (Figure 2) and to plot the interaction indicator,  $\rho_w$ , as a function of the distance from the distractor to the center of the neuron’s

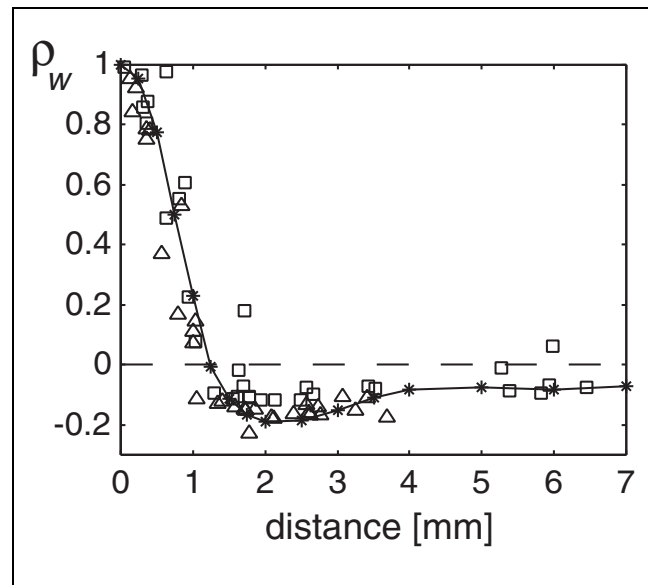


**Figure 2.** The relative interaction strength between neurons defined as the value of the distractor-related buildup discharge relative to the buildup activity without a distractor and normalized to the maximal value of distractor enhancement. Shown are data from two cells, one cell (squares) that responds maximally to a distractor at  $R = -19.4^\circ$ ,  $\Phi = -33.4^\circ$ , and another cell (triangles) that responds maximally to a distractor at  $R = 1.7^\circ$ ,  $\Phi = 57.7^\circ$ . The distance is defined in relation to these preferred directions. The asterisks, which are interpolated by a line, represent the corresponding simulations of the model.



response field. We used, in the following, the location of maximum  $\rho_w$  with values ( $R = -19.4^\circ$ ,  $\Phi = -33.4^\circ$ ; Figure 2, squares) and ( $R = 1.7^\circ$ ,  $\Phi = 57.7^\circ$ ; Figure 2, triangles), respectively, as estimates of the center of the response fields (shown as white dots in Figure 1D). The “distance” in Figure 2 is measured from these locations, and the values of the interaction indicators  $\rho_w$  are normalized to the values of maximal  $\rho_w$  for each cell separately. The relative similarity of the interaction patterns extracted from these two neurons located at different collicular locations on the motor map compares well with the assumption in our model of a translation invariant effective interaction profile within the SC, and the form of the data verify our assumption of the corresponding form with short-distance excitation and long-distance inhibition.

This effective profile of distractor interaction, however, does not provide a direct measurement of the synaptic efficacy. Rather, it is the sum over all cell activities in the layer multiplied with the individual synaptic efficacy. To quantify this interaction in our model (using the parameterization introduced in Equation 7), we chose values for the parameters of the interaction matrix so that simulated distractors have similar effects on the buildup activity of buildup nodes as did real distractors upon real neural activity in the monkey experiments. The model simulation of the distractor effect, with the weight matrix parameters used throughout this study, is illustrated by the solid line in Figure 2.

### *Influence of Distractors on SRTs*

In a distractor experiment, subjects are required to ignore the distractor. However, when a distractor is presented in close temporal relation with the target, it has a pronounced effect on the SRTs (see also, Walker et al., 1997; Corneil & Munoz, 1996). The SRTs can be noticeably faster, compared with the control condition of no distractor, when a distractor appears near to the position of the target. In contrast, a distractor in the opposite hemifield can increase SRTs considerably.

Our simulations illustrate that distractor effects can be a direct consequence of the exogenous modulation of surrounding neurons in the SC (compare upper and lower panels in Figure 1B). As we have seen, remote distractors reduce the activity of all distant neurons including those coding for the target saccade (right panel of Figure 1B) resulting in a prolonged SRT, whereas near distractors enhance the activity of neurons coding for the target saccade (middle panel of Figure 1B) facilitating SRTs. In Figure 3A, we show SRTs for simulations without distractors and with distractors presented 50 msec before target appearance. In the simulation, distractors were presented at the same position ( $u = -2.5$  mm) as the simulated target location (near distractor), which was also the preferred direction of the recorded node, and at a location corresponding to a

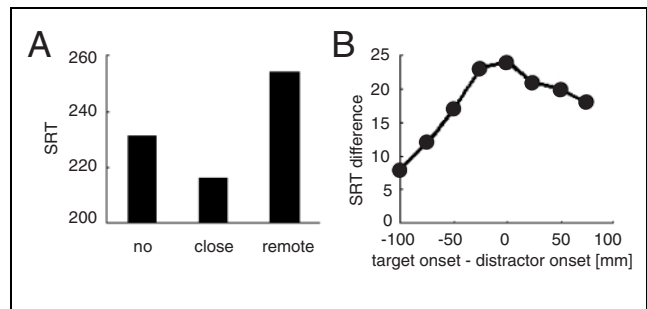


**Figure 3.** (A) Simulated SRTs in the distractor paradigm with a 50-msec disparity between distractor and target onsets. Shown are simulation data for SRTs without distractor (no), for a near distractor presented at the same position as target (close), and for a distractor with receptive field 2 mm distant from the receptive field of the target (remote). (B) Difference between SRT during the remote distractor condition and the no distractor condition (distractor minus no distractor) for distractors presented at various times in relation to the appearance of the target.

collicular distance of 2 mm from the recorded buildup node (remote distractor). The behavior of these simulated SRTs resembles well the average behavior of human subjects in distractor experiments (Walker et al., 1997; Corneil & Munoz, 1996).

Another contributing factor modulating SRTs in the distractor paradigm, besides the spatial proximity of distractor and target, is the temporal relation of the two cues. It is only in a short temporal window, determined by the transient effect of the distractor signal and the dynamics of the buildup layer, that the distractor will influence the dynamics of saccade initiation (Walker et al., 1997). In Figure 3B, we display the retarding effect within our model simulations of a remote distractor presented in various temporal relations to the appearance of the target. The visual amplitude was set to  $a_{\text{exo}} = 50$  in these simulations. The SRT was greatest when the remote distractor was displayed in close temporal proximity with the target.

Besides this dynamic influence of distractors on SRTs via collicular interactions, it should be noted that a distractor that precedes target appearance by a sufficient duration can also serve as a warning signal that might increase alertness and decrease temporal uncertainty about target presentation. Thus, when a distractor stimulus (whether visual or auditory) can be used to predict the time of target onset, SRTs can be reduced independently of the location of the distractor (Taylor et al, 1998; Walker et al., 1997). Such SRT reductions were also found in monkey experiments (Dorris, Olivier, & Munoz, unpublished observations). In these cases, the nondependence of the SRTs on the location of a visual or auditory (Corneil & Munoz, 1996) distractor demonstrates that this warning effect has, like the fixation offset effect, global consequences for saccadic performance. What has not been done yet is to teach the monkey that an auditory signal reliably predicts the time of target and

then record from SC neurons to see if these reductions are mediated by a reduction in fixation activity following the auditory event (what Taylor et al, 1998 refer to as endogenous fixational disengagement).

### Antisaccades

In the antisaccade task, subjects must move their eyes to a location that is opposite to that of the stimulus (Everling & Fischer, 1998; Hallett, 1978). Human behavioral data collected by Forbes and Klein (1996) are shown in Figure 4A. Considering correct saccadic responses only, subjects are slower at initiating antisaccades compared with prosaccades. In addition, the gap/overlap effect is reduced in the antisaccade paradigm; the subjects were on average 51 msec slower in the overlap condition compared to the gap condition in the prosaccade task, whereas this difference was only 31 msec in the antisaccade task.

Both of these effects are inherent in our model as can be seen in the simulation results (Figure 4B). The antisaccades consistently had longer SRTs than prosaccades. In addition, the difference between SRTs in the overlap condition versus gap condition was 48 msec in the prosaccade task and only 18 msec in the antisaccade task. In these simulations, we used an initial endogenous amplitude  $a_{\text{endo}} = 7$ , set the fixation offset to  $a_{\text{exo}} = -5$ , and increased the exogenous amplitude slightly to  $a_{\text{exo}} = 70$ . The gap and overlap intervals in both the human performance experiments and the simulations were 200 msec.

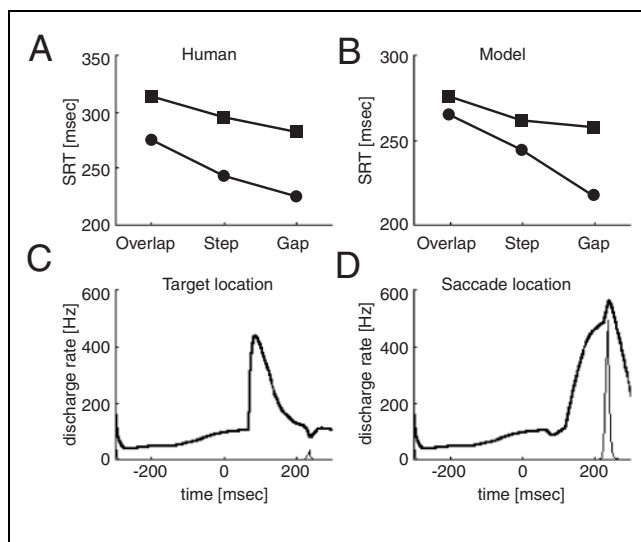


**Figure 4.** Upper row: SRTs for prosaccades (circles) and antisaccade (squares) within the overlap, step, and gap condition. (A) Human performance data from Forbes and Klein (1996), (B) Model simulation. Lower row: Simulated model node activities for buildup nodes (thick line) and burst nodes (thin line) in an antisaccade task within the gap condition; (C) for a node with a response field corresponding to the target location, (D) for a node with a response field corresponding to the saccade location.

It is instructive to see how the prolonged SRTs for antisaccades compared to prosaccades are produced within our model. In the prosaccade task, the exogenous signal triggers cell activity at the location to which the saccade should be made. This activity is then consistent with, and thus facilitates, the buildup initiated by an endogenous signal at the same location. This is contrary to antisaccades where no such facilitating exogenous activity is present. Instead, the exogenous input arrives at the stimulated location (Figure 4C) and not at the location to which the antisaccade must be made (Figure 4D). Thus, in the antisaccade task, the exogenous signal is also a remote distractor with respect to the required response (and endogenous input). These activity profiles of our model nodes are similar to the activity profiles of cells recorded from the SC of monkeys in the antisaccade task (Everling, Dorris, Klein, & Munoz, 1999; Everling, Dorris, & Munoz, 1998).

It is thus interesting to note that the exogenous visual signal in the antisaccade task has a similar effect to that seen with a remote distractor. The sudden appearance of the exogenous stimulus reduces buildup activity at all remote locations (see Figure 2), which includes the location required to initiate the saccade, adding to the time required for the endogenous input to build up the necessary activity to initiate the antisaccade. The prolonged time needed for the initiation of an antisaccade relative to a prosaccade also reduces the effect of the fixation offset. This in turn reduces the SRT differences in the overlap versus gap condition, as can be seen in the human performance as well as simulated data.

### Target Location Probability

To study the effect of varying the location-specific endogenous context within which an exogenous signal is presented, we designed an experiment wherein a target could appear at one of two possible locations in opposite areas of the visual field within an otherwise standard prosaccade task. The probability of the appearance of the target at one location was set to be larger than at the other possible location. In the following experiments, the target appeared in 80% of the trials at the more likely location, whereas the target appeared in only 20% of the trials at the opposite location. SRTs of human subjects in such experiments are shown in Figure 5A (Simpson & Klein, 1997). The gap and overlap intervals were fixed to 200 msec. Our behavioral experiments revealed that SRTs of human subjects were faster when the more likely target was presented and thus the expected saccade was made (Figure 5A, squares) than when unexpected saccades were made (to the less likely target) (Figure 5A, circles). Furthermore, the difference between the SRTs to the likely and unlikely target was consistently greater in the gap condition compared to the step and overlap conditions.

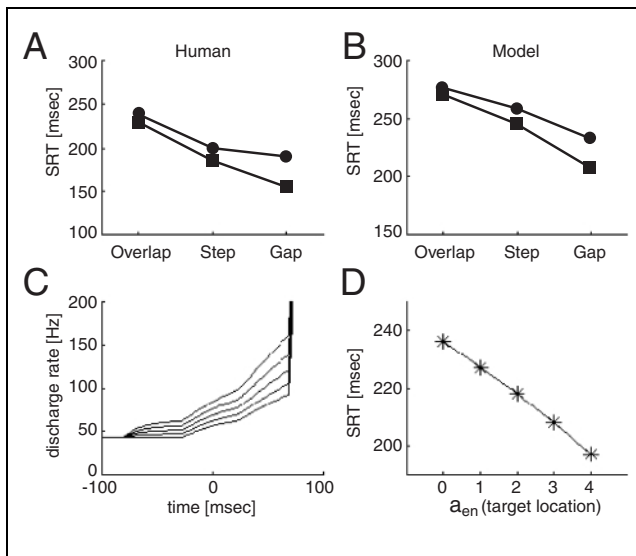


**Figure 5.** Gap/overlap effect for targets with different probabilities of appearance. (A) SRTs of human subjects saccading to two possible target locations. SRTs to a location at which the target appeared in 80% of the trials are shown as squares, whereas SRTs to the less likely location in which the target appears 20% of the trials are shown as circles (from Simpson et al., 1997). (B) Corresponding simulated SRTs with (squares) and without (circles) endogenous input prior to the target based on target location probability. (C) Simulated buildup activities with different levels of pretarget endogenous input ( $a_{en} = 0, 1, 2, 3, 4$ ). The corresponding SRTs are shown in (D).

In our simulations, we model the target probability information as a weak pretarget endogenous input at the more likely target location. This endogenous probability amplitude was thereby set to  $a_{endo} = 3$  at  $-200$  msec before target appearance. This was the same level as the amplitude of the central endogenous signal during the gap interval. The exogenous amplitude was set to  $a_{exo} = 50$ . Results for the simulations of SRTs with a 100-msec overlap of fixation and target, within the step condition, as well as a 100-msec gap interval are shown in Figure 5B. The simulated data reflects well the effect in human behavior. Similar findings have been reported previously by our group (Trappenberg et al., 1997) with a different set of parameters, illustrating the stability of these findings.

Essential in our proposed mechanism leading to shorter SRTs to the more likely target is that the additional endogenous signal is integrated before target appearance.<sup>2</sup> This information leads to an enhanced buildup of activity at the more likely target location compared to the less likely target location. This pretarget buildup is most pronounced in a gap condition because removal of the fixation inhibition allows a greater buildup than in the overlap condition. The buildup of activity in the gap condition is shown in Figure 5C for different values of the amplitude  $a_{endo}$  of the pretarget endogenous signal at the target location (local preparation). Similar behavior was found in neuronal recordings obtained from buildup neurons in the monkey SC (Basso & Wurtz,

1998; Dorris & Munoz, 1998). In our model, simulated saccadic latencies decrease as the amplitude of endogenous pretarget activity increases (Figure 5D); a prediction that is confirmed by Dorris and Munoz (1998, Figure 8B). Examination of SRTs as a function of target location probability, manipulated parametrically, would provide useful converging evidence.

### Express Saccades

Finally, we outline a possible source of bimodal distributions of SRTs. The fast components of these distributions have been referred to as “express” because they have much shorter SRTs compared to those of the slower mode representing regular saccades (Paré & Munoz, 1996; Fischer & Weber 1993; Fischer & Boch, 1983; but see Kingstone & Klein, 1993).

In the simulations of the paradigms discussed so far, we have suppressed the noise term in the motor dynamics (Equation 2). Noise represents the stochastic nature of brain processes. The noise term in Equation 2 was included to represent possible stochastic processing in the motor layer itself, as well as possible variability in the input signals. A reasonable amount of this noise will not alter the results of the paradigms discussed so far and was therefore not included in the simulations shown in the preceding figures in order to illustrate more clearly the principle form of node activities. However, some variability in processing is instrumental in the generation of distributions of SRT. Hence, we included noise in the simulation presented in this section.

SRTs depend critically on the level of buildup activity, which in turn is driven by the values of exogenous (e.g., fixation removal) and endogenous (preparatory) input. Variability in these driving sources will lead to some variability in SRTs. The form of the resulting distribution of SRTs depends, however, on the dynamics of the motor layer. Our goal in this section is to demonstrate that the dynamics of the motor layer can thereby produce bimodal SRT distributions from a unimodal noise source.

In the simulations, we used visual amplitudes of  $a_{exo} = 55$  and a central endogenous fixation amplitude of  $a_{endo} = 3$  as well as a peripheral, target location-specific endogenous amplitude of  $a_{endo} = 2$ . The gap period was set to 200 msec. We included noise with a strength factor of  $a_{\eta} = 20$ . The resulting distribution of simulated SRTs for 383 trials reveal two modes (Figure 6A): a later mode of SRTs typically observed in our simulations, and an earlier mode, reminiscent of express saccades. The activity level of a node on a simulated trial with regular SRT is displayed in Figure 6B. This resembles the behavior of saccade initiation within the gap paradigm illustrated earlier for both model and real neurons (compare to leftmost panels of Figure 1B). However, the mechanism underlying the fast mode (express saccades) is evident in Figure 6C, which shows

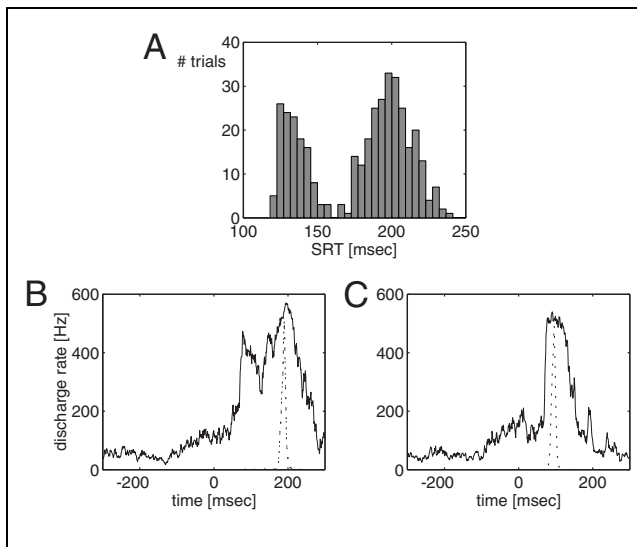


**Figure 6.** Simulated SRTs and activity levels in a 200-msec gap condition when noise is included in the model. Zero on the time-axis corresponds to the time of target presentation. (A) Distribution of SRTs in 383 trials. (B,C) The solid line represents the activity of the buildup node at the target location; the dotted line represents the activity of a burst node in this vicinity. Note that due to efferent delay, saccades are initiated approximately 20 msec after the burst. (B) Example of trial with regular SRT (211 msec). (C) Example of trial with short SRT (117 msec) where the exogenous peak initiated a saccade.

the activity level of the same node on a simulated trial with short SRT. The fluctuations are large enough so that the visual peak sometimes generates the saccade. This parallels the motor preparation hypothesis for express saccade generation (Dorris et al., 1997; Paré & Munoz, 1996), which suggests that increased buildup activity in advance of target presentation may allow the visual burst to surpass the threshold for eliciting a saccade. If there is not enough buildup activity in advance of target presentation, the visual burst does not surpass this threshold and a subsequent motor burst must occur later in time (Dorris et al., 1997; Edelman & Keller, 1996). Bimodal SRT distributions in the gap condition have led some investigators (e.g., see Fischer & Weber, 1993) to hypothesize that the saccades from different modes are produced through essentially different neural pathways. Our demonstration, that bimodal SRT distributions can be produced entirely by the characteristics of collicular processes, provides a simulation-based challenge to multiple pathway explanations of bimodality.

## DISCUSSION

Computational models of behavioral phenomena, like those we have explored here, are explicitly designed to predict or generate the target behavior. We refer to this feature as the model's sensitivity to "top-down" constraints. Partly because a multitude of such models can be formulated to produce a particular behavioral pattern

and partly because cognitive neuroscience seeks to understand how behavior is implemented in the brain, whenever possible, such models ought also be sensitive to the "bottom-up" constraints of generating the behavior of the neurons thought to be responsible for the target behavior (Trappenberg & Klein, 1999). The strength of our model is that it accurately simulates a variety of oculomotor (behavioral) phenomena while also simulating the underlying neuronal behavior.

The intermediate layers of the SC receive convergent input from many cortical and subcortical sources involved in saccade generation (Sparks & Hartwich-Young, 1989). This integration is often reflected in models with a winner-take-all component. Kopecz (1995) and Kopecz and Schöner (1995) first realized that a dynamic integration of exogenous and endogenous signals could explain the SRT reduction associated with the gap effect. They termed this dynamic component "readiness dynamics" and proposed a description of this dynamic using neural fields of the type studied by Amari (1977). Here, we take this approach a step further by arguing that this readiness dynamic is indeed realized in the primate SC. Hence, modifications of the model by Kopecz and Schöner have been made to reflect more directly physiological constraints including a close comparison of behavioral and cell data in a broad range of paradigms.

It is important to note that our model exhibits a direct correspondence to that of Arai et al. (1994). Both models equivalently implement a collicular map with a laterally interacting layer of model cells. Arai et al. adjusted the lateral weights of the motor layer by training the network to reproduce the spatio-temporal activity pattern in the SC. They found an interaction matrix that depends only on the distance between the nodes and which exhibits short-distance excitatory and long-range inhibitory values resembling the interaction matrix used in this study. In this article, we provide additional, direct and independent support for this form of collicular interactions from cell data and behavior studies. Unlike the model by Arai et al., we have not implemented a burst generator module (Scudder, 1988; Van Gisbergen et al., 1981), nor do we include a negative feedback loop to control saccade accuracy (Optican, 1995; Arai et al., 1994; Massone, 1994; Lefèvre & Galiana, 1992) as we are more interested in the dynamics of saccade initiation than in the metrics and dynamics of the movements themselves.

We believe that our model of the dynamics of saccade initiation is compatible with more global models of the oculomotor system that include other cortical and subcortical areas (see, e.g., Lefèvre, Quaia, & Optican, 1998; Grossberg, Roberts, Aguilar, & Bullock, 1997; Dominey & Arbib, 1992). The inclusion of computational machinery outside the SC in these models was required to account for memory-guided saccades and some aspects of target selection that in our framework are included in

our control of endogenous signals. One of the most advanced models of the saccade-generating system itself, including the SC, is the model by Grossberg et al. (1997). These authors focus in particular on the generation and translation of representations of the visual world, and are able to account for several adaptive effects within their model. We do not focus on adaptive effects in this article, but instead, concentrate on particular aspects in the dynamic of saccade initiation. It would be interesting to see if the intra-collicular interaction structure proposed in this article can emerge within the model by Grossberg et al. (1997).

The interaction structure was probed with a unique new method using single cell recordings in a paradigm with distractors. The results of these experiments are consistent with an interaction structure characterized by excitatory interactions between collicular areas with anatomical distances less than around 1 mm, and inhibition between more remote collicular sites. This is consistent with anatomical and physiological findings (Meredith & Ramoa 1998; Munoz & Istvan, 1998; Olivier et al., 1998; Behan & Kime 1996; Mize et al., 1991; McIlwain 1982), and also resembles the interaction profile found by Arai et al. (1994).

The mechanisms leading to the effects discussed in this article are simple enough to provide a satisfactory understanding and analysis of several aspects of saccadic initiation. Various inputs compete within the SC through lateral interactions. The corresponding dynamics of this competition account for several SRT effects. We found it useful to classify the inputs to the SC into exogenous (direct visually guided) and endogenous (voluntary or intentional). This scheme is useful in the classification of behavioral effects, and can also be given concrete meaning in brain mechanisms. Visual (exogenous) information reaches the intermediate layers of the SC within around 70 msec in monkeys after appearance of visual stimuli and is always location-specific. These signals, which are transient in nature, represent a lower form of visual information processing. Meaning can be attached to these signals with further (presumably cortical) processing. Such stimulus-based endogenous information reaches the SC only after an additional delay. In contrast, voluntary preparation of a saccade can be implemented by endogenous activation before the appearance of a stimulus (exogenous input).

Location-specific activity of buildup cells from separate exogenous and endogenous sources are present in the antisaccade task. Activity related to instructional (endogenous) information is seen at the site corresponding to the saccade location. However, activity related to the visual target (exogenous) occurs at the opposite collicular location. We have shown that the influence of isolated exogenous responses on collicular map dynamics can be studied by using distractor experiments.

The influence of endogenous factors on collicular map dynamics was also studied with a paradigm including several possible targets with different probabilities of appearance. To date, most studies of saccade initiation effects have not attempted to distinguish between the different mechanisms classified in our scheme and therefore, present a mixture of these effects. An example is the gap/overlap effect, which has endogenous as well as exogenous components. Although this effect is mainly determined by global mechanisms, depending on experimental conditions, it can also have location-specific components. For example, if the target location or time of appearance is not randomized, there can be an endogenous location-specific component, facilitating the generation of express saccades.

Further evidence for the involvement of lateral excitation and remote inhibition in saccade generation is found in studies of averaging saccades produced by two-point electrical stimulation in the SC (Van Opstal & Van Gisbergen, 1989; Robinson, 1972). Behavioral findings have shown that averaging saccades tend to occur when two targets are in close proximity (for recent examples, see Chou, Sommer, & Schiller, 1999; Edelman & Keller, 1998; Walker et al., 1997). As the angular distance between the targets is increased, the percentage of averaging saccades observed is diminished (Chou et al., 1999). Additional findings have revealed that when two target stimuli are presented in close proximity, averaging saccades occur at short latencies (i.e., express saccade range), while longer latency saccades do not average (Chou et al., 1999; Edelman & Keller, 1998). Of particular interest here is that the movement fields of individual saccade-related neurons in the intermediate layers of the SC were larger in size for averaging saccades (Edelman & Keller, 1998) suggesting that lateral interactions at the level of the SC may play an important role in the generation of averaging saccades.

Our model also makes specific predictions regarding the effects of local inactivation of populations of neurons on the SC motor map. Such pharmacological manipulations (Davidson, Everling, Lablans, & Munoz, 1999; Aizawa & Wurtz, 1998; Munoz & Wurtz, 1993; Schiller, Sandel, & Maunsell, 1987; Hikosaka & Wurtz, 1985) lead to changes in the SRT. A future step in model development will be to try to accommodate these results by removing subsets of elements within the dynamic layer of the SC. We predict that removal of the fixation elements will make the model unstable thereby producing many premature or unwanted saccades. In addition to undertaking such direct tests of the model, we also plan to increase the range of behavioral paradigms that can be simulated with the simple SC model, and to begin to characterize the contributions of cortical and subcortical systems to the programming, initiation, and execution of saccadic eye movements.

As mentioned above, we have demonstrated that a set of parameters exists such that various behavioral and cell

pattern can be modeled. A further question is how these parameters are adjusted by nature. For example, we have mentioned in the discussion of express saccades that the levels of endogenous and exogenous inputs have to be in a certain range in order to display bimodal distributions. Express saccades are strongly influenced by learning (Paré & Munoz, 1996), and it is hence interesting to search for the corresponding neural mechanisms. We are currently exploring various extensions of our model in this direction.

## Acknowledgments

This research was supported by an NSERC (Canada) Collaborative Project Grant to R. M. Klein, D. P. Munoz, T. P. Trappenberg, and P. A. McMullen. D. P. Munoz is a scientist of the Medical Research Council of Canada. We would like to acknowledge the valuable contributions of Sol Simpson during an earlier phase of this project (Simpson, Klein, & Trappenberg, 1998) and to thank the RIKEN Brain Sciences Institute for supporting Dr. Trappenberg while he was working on the simulations reported in this manuscript.

Reprint requests should be sent to Raymond M. Klein, Department of Psychology, Dalhousie University, Halifax, Nova Scotia B3H 4J1, Canada. E-mail: ray.klein@dal.ca.

## Notes

1. Because a report describing neural activity during the distractor paradigm is in preparation, it is not appropriate to make a fuller presentation of those findings here. Suffice it to say that Olivier et al. have recorded from about 40 neurons in this paradigm and the two whose data are illustrated in Figure 1D are representative.

2. An alternative mechanism might be proposed: The more likely target could give rise to a stronger endogenous target signal. Although such a mechanism might be operating along with the endogenous pretarget signal we have hypothesized, the proposal that on its own it might account for the effect of target probability can be easily dismissed. First, the advantage for likely targets would be equivalent in all gap/overlap conditions leading to a global shift of the SRT curve. However, this is not what is seen (Figure 5A). More directly, Dorris and Munoz (1998) have reported that pretarget buildup activity is sensitive to target location probability.

## REFERENCES

Aizawa, H., & Wurtz, R. H. (1998). Reversible inactivation of monkey superior colliculus: I. Curvature of saccadic trajectory. *Journal of Neurophysiology*, *79*, 2082–2096.

Amari, S. (1977). Dynamics of pattern formation in lateral-inhibition type neural fields. *Biological Cybernetics*, *27*, 77–87.

Arai, K., Keller, E. L., & Edelman, J. A. (1994). Two-dimensional neural network model of the primate saccade system. *Neural Networks*, *7*, 1115–1135.

Basso, M. A., & Wurtz, R. H. (1998). Modulation of neural activity in superior colliculus by changes in target probability. *Journal of Neuroscience*, *18*, 7519–7534.

Behan, M., & Kime, N. M. (1996). Intrinsic circuitry in the deep layers of the cat superior colliculus. *Visual Neuroscience*, *13*, 1031–1042.

Carpenter, R. H., & Williams, M. L. (1995). Neural computation of log likelihood in control of saccadic eye movements. *Nature*, *377*, 59–62.

Chou, I., Sommer, M. A., & Schiller, P. H. (1999). Express averaging saccade in monkeys. *Vision Research*, *39*, 4200–4216.

Corneil, B. D., & Munoz, D. P. (1996). The influence of auditory and visual distractors on human orienting gaze shifts. *Journal of Neuroscience*, *16*, 8193–8207.

Davidson, M. C., Everling, S., Lablans, A., & Munoz, D. P. (1999). Comparison of pro- and antisaccades in primates: III. Reversible activation/inactivation of frontal eye field and superior colliculus. *Society of Neuroscience Abstracts*, *25*, 367.

Desimone, R., & Duncan, J. (1995). Neural mechanisms of selective visual attention. *Annual Review of Neuroscience*, *18*, 193–222.

Dominey, P. F., & Arbib, M. A. (1992). A cortico-subcortical model for generation of spatially accurate saccades. *Cerebral Cortex*, *2*, 153–174.

Dorris, M. C., & Munoz, D. P. (1995). A neural correlate for the gap effect on saccadic reaction times in monkey. *Journal of Neurophysiology*, *73*, 2558–2562.

Dorris, M. C., & Munoz, D. P. (1998). Saccadic probability influences motor preparation signals and time to saccadic initiation. *Journal of Neuroscience*, *18*, 7015–7026.

Dorris, M. C., Paré, M., & Munoz, D. P. (1997). Neural activity in monkey superior colliculus related to the initiation of saccadic eye movements. *Journal of Neuroscience*, *17*, 8566–8579.

Dorris, M. C., Paré, M., & Munoz, D. P. (2000). Immediate neural plasticity shapes motor performance. *Journal of Neuroscience*, *20*, RC52 1 of 5.

Edelman, J. A., & Keller, E. L. (1996). Activity of visuomotor burst neurons in the superior colliculus accompanying express saccades. *Journal of Neurophysiology*, *76*, 908–926.

Edelman, J. A., & Keller, E. L. (1998). Dependence on target configuration of express saccade-related activity in the primate superior colliculus. *Journal of Neurophysiology*, *80*, 1407–1426.

Everling, S., Dorris, M. C., Klein, R. M., & Munoz, D. P. (1999). Role of primate superior colliculus in preparation and execution of anti-saccades and pro-saccades. *Journal of Neuroscience*, *19*, 2740–2754.

Everling, S., Dorris, M. C., & Munoz, D. P. (1998). Reflex suppression in the anti-saccade task is dependent on prestimulus neural processes. *Journal of Neurophysiology*, *80*, 1584–1589.

Everling, S., & Fischer, B. (1998). The antisaccade: A review of basic research and clinical studies. *Neuropsychologia*, *36*, 885–899.

Fischer, B., & Boch, R. (1983). Saccadic eye movements after extremely short reaction times in the monkey. *Brain Research*, *260*, 21–26.

Fischer, B., & Weber, H. (1993). Express saccades and visual attention. *Behavioral and Brain Sciences*, *16*, 553–610.

Forbes, K., & Klein, R. M. (1996). The magnitude of the fixation offset effect with endogenously and exogenously controlled saccades. *Journal of Cognitive Neuroscience*, *8*, 344–352.

Grossberg, S., Roberts, K., Aguilar, M., & Bullock, D. (1997). A neural model of multimodal adaptive saccadic eye movement control by superior colliculus. *Journal of Neuroscience*, *17*, 9706–9725.

Hallett, P. E. (1978). Primary and secondary saccades to goals defined by instructions. *Vision Research*, *18*, 1279–1296.

Hikosaka, O. (1989). Role of basal ganglia in saccades. *Review of Neurology (Paris)*, *145*, 580–586.

Hikosaka, O., & Wurtz, R. H. (1985). Modification of saccadic

- eye movements by GABA-related substances: I. Effect of muscimol and bicuculine in monkey superior colliculus. *Journal of Neurophysiology*, 53, 266–291.
- Istvan, P. J., Dorris, M. C., & Munoz, D. P. (1994). Functional identification of neurons in the monkey superior colliculus that project to the paramedian reticular formation. *Society of Neuroscience Abstracts*, 20, 141.
- Jancke, D., Erlhagen, W., Dinse, H. R., Akhavan, M., Giese, M., & Schöner, G. (1999). Parametric representation of retinal location: Neural population dynamics and interaction in cat visual cortex. *Journal of Neuroscience*, 19, 9016–9028.
- Kingstone, A., & Klein, R. M. (1993). What are human express saccades? *Perception and Psychophysics*, 54, 260–273.
- Klein, R. M., Kingstone, A., & Pontefract, A. (1992). Orienting of visual attention. In K. Rayner (Ed.), *Eye movements and visual cognition: Scene perception and reading*, (pp. 46–67). New York: Springer-Verlag.
- Klein, R. M., & Pontefract, A. (1994). Does oculomotor readiness mediate cognitive control of visual attention? Revisited! In C. Umiltà & M. Moscovitch (Eds.), *Attention and performance: XV. Conscious and unconscious processing*, (pp. 333–350). Cambridge: MIT Press.
- Klein, R. M., & Shore, D. I. (2000). Relationships among modes of visual orienting. In S. Monsell & J. Driver (Eds.), *Attention and performance: XVIII. Control of cognitive processes*, (pp. 195–208). Cambridge: MIT Press.
- Konen, W. K., Maurer, T., & von der Malsburg, Ch. (1994). A fast dynamic link matching algorithm for invariant pattern recognition. *Neural Networks*, 7, 1019–1030.
- Kopecz, K. (1995). Saccadic reaction time in gap/overlap paradigm: A model based on integration of intentional and visual information on neural, dynamic fields. *Vision Research*, 35, 2911–2925.
- Kopecz, K., & Schöner, G. (1995). Saccadic motor planning by integrating visual information and expectation on neural dynamic fields. *Biological Cybernetics*, 73, 49–60.
- Lefèvre, P., & Galiana, H. L. (1992). Dynamic feedback to the superior colliculus in a network model of the gaze control system. *Neural Networks*, 5, 871–900.
- Lefèvre, P., Quaia, Ch., & Optican, L. M. (1998). Distributed model of control of saccades by superior colliculus and cerebellum. *Neural Networks*, 11, 1175–1190.
- Massone, L. E. (1994). A neural-network for control of eye movements: Basic mechanisms. *Biological Cybernetics*, 70, 293–304.
- McIlwain, J. T. (1982). Lateral spread of neural excitation during microstimulation in intermediate gray layer of cat's superior colliculus. *Journal of Neurophysiology*, 47, 167–178.
- Meredith, M. A., & Ramoa, A. S. (1998). Intrinsic circuitry of the superior colliculus: Pharmacophysiological identification of horizontally oriented inhibitory interneurons. *Journal of Neurophysiology*, 79, 1597–1602.
- Milner, A. D., & Goodale, M. A. (1995). *The visual brain in action*. Oxford: Oxford University Press.
- Mize, R. R., Jeon, C. J., Hamada, O. L., & Spencer, R. F. (1991). Organization of neurons labeled by antibodies to gamma-aminobutyric acid (GABA) in the superior colliculus of the rhesus monkey. *Vision Research*, 6, 75–92.
- Moschovakis, A. K. (1996). The superior colliculus and eye movement control. *Current Opinions in Neurobiology*, 6, 811–816.
- Munoz, D. P., & Istvan, P. J. (1998). Lateral inhibitory interactions in the intermediate layers of the monkey superior colliculus. *Journal of Neurophysiology*, 79, 1193–1209.
- Munoz, D. P., & Wurtz, R. H. (1993). Fixation cells in monkey superior colliculus: I. Characteristics of cell discharge. *Journal of Neurophysiology*, 70, 559–575.
- Munoz, D. P., & Wurtz, R. H. (1995a). Saccade related activity in monkey superior colliculus: I. Spread of activity during saccades. *Journal of Neurophysiology*, 73, 2334–2349.
- Munoz, D. P., & Wurtz, R. H., (1995b). Saccade related activity in monkey superior colliculus: II. Characteristics of burst and buildup cells. *Journal of Neurophysiology*, 73, 2313–2333.
- Olivier, E., Dorris, M. C., & Munoz, D. P. (1999). Lateral interactions in the superior colliculus, not an extended fixation zone, can account for the remote distractor effect. *Behavioral and Brain Sciences*, 22, 694–695.
- Olivier, E., Porter, J. D., & May, P. J. (1998). Comparison of the distribution and somatodendritic morphology of tectotectal neurons in the cat and monkey. *Visual Neuroscience*, 15, 903–922.
- Optican, L. M. (1995). A field theory of saccade generation: Temporal-to-spatial transformation in the superior colliculus. *Vision Research*, 35, 3313–3320.
- Paré, M., & Munoz, D. P. (1996). Saccadic reaction time in the monkey: Advanced preparation of oculomotor programs is primarily responsible for express saccade occurrence. *Journal of Neurophysiology*, 76, 3666–3681.
- Posner, M. I. (1980). Orienting of attention. *Quarterly Journal of Experimental Psychology*, 32, 3–25.
- Ratcliff, R., Van Zandt, T., & McKoon, G. (1999). Connectionist and diffusion models of reaction time. *Psychological Review*, 106, 261–300.
- Reuter-Lorenz, P. A., Hughes, H. C., & Fendrich, R. (1991). The reduction of saccadic latency by prior offset of the fixation point: An analysis of the “gap effect”. *Perception and Psychophysics*, 49, 167–175.
- Robinson, D. A. (1972). Eye movements evoked by collicular stimulation in the alert monkey. *Vision Research*, 12, 1795–1808.
- Ross, S. M., & Ross, L. E. (1981). Saccadic latency and warning signals: Effects of auditory and visual stimulus onset and offset. *Perception and Psychophysics*, 29, 429–437.
- Samsonowich, A., & McNaughton, B. L. (1997). Path integration and cognitive mapping in a continuous attractor neural network model. *Journal of Neuroscience*, 17, 5900–5920.
- Saslow, M. G. (1967). Saccade latency and warning signals: Stimulus onset, offset and change as warning events. *Journal of the Optical Society of America*, 57, 1024–1029.
- Schiller, P. H., Sandel, J. H., & Maunsell, J. H. R. (1987). The effect of frontal eye field and superior colliculus lesions on saccadic latencies in the rhesus monkey. *Journal of Neurophysiology*, 57, 1033–1049.
- Schiller, P. H., & Wurtz, R. H. (1975). Sensorimotor transformation in the tectum of the macaque. *Neuroscience Research Program Bulletin*, 13, 226–228.
- Scudder, C. A. (1988). A new local feedback model of saccadic burst generation. *Journal of Neurophysiology*, 59, 1455–1474.
- Simpson, S., & Klein, R. M. (1997). *On the interaction between endogenous and exogenous contributions to saccadic programming*. Presented at the Annual Meeting of the Psychonomics Society, Philadelphia.
- Simpson, S. D., Klein, R. M., & Trappenberg, T. P. (1998). *Simulating oculomotor behavior within a neural field model*. Poster presented at the Cognitive Neuroscience Society, San Francisco.
- Simpson, S., Trappenberg, T., Klein, R. M., & McMullen, P. (1997). *Saccadic reaction time as a function of target location probability and the gap effect*. Presented at the Annual Meeting of the Cognitive Neuroscience Society. Boston, MA.
- Sparks, D. L. (1978). Functional properties of neurons in the monkey superior colliculus: coupling of neuronal activity and saccade onset. *Brain Research*, 156, 1–16.

- Sparks, D. L., & Hartwich-Young, R. (1989). The deep layers of the superior colliculus. In R. H. Wurtz & M. E. Goldberg (Eds.), *The neurobiology of saccadic eye movements* (pp. 213–255). Amsterdam: Elsevier.
- Taylor, J. G. (1999). Neural bubble dynamics in two dimensions: I. Foundations. *Biological Cybernetics*, *80*, 393–409.
- Taylor, J. G., & Alavi, F. N. (1995). A global competitive neural network. *Biological Cybernetics*, *72*, 233–248.
- Taylor, J. G., & Alavi, F. N. (1997). A global competitive model for attention. *Neural Network World*, *5*, 477–502.
- Taylor, T. L., Kingstone, A., & Klein, R. M. (1998). Visual offsets and oculomotor disengagement: Endogenous and exogenous contributions to the gap effect. *Canadian Journal of Experimental Psychology*, *52*, 192–200.
- Trappenberg, T. P. (1998a). *A model of the superior colliculus with competing and spiking neurons*. BSIS Technical Report, 98-93.
- Trappenberg, T. P. (1998b). *Dynamic cooperation and competition in a network of spiking neurons*. Proceedings ICONIP'98, Kitakushu, Oct. 1998.
- Trappenberg, T. P., & Klein, R. M. (1999). Generating oculomotor and neuronal behavior in a neural field model of the superior colliculus. *Behavioral and Brain Sciences*, *22*, 700–701.
- Trappenberg, T. P., Simpson, S., Klein, R. M., McMullen, P., Munoz, D. P., & Dorris, M. C. (1997). *Neural field model of oculomotor preparation and disengagement* (vol. 1, pp. 591–596). Proceedings of WCNN'97 in Huston 1997.
- Ungerleider, L. G., & Mishkin, M. (1982). Two cortical visual systems. In D. J. Ingle & M. A. Goodale, R. J. W. Mansfield (Eds.), *Analysis of visual behavior*. Cambridge: MIT Press.
- Usher, M., Stemmler, M., Koch, Ch., & Olami, Z. (1996). Network amplification of fluctuations causes high spike rate variability, fractal firing patterns and oscillatory local field potentials. *Neural Computation*, *6*, 795–836.
- Van Gisbergen, J. A. M., Robinson, D. A., & Gielen, S. (1981). A quantitative analysis of generation of saccadic eye movements by burst neurons. *Journal of Neurophysiology*, *45*, 417–422.
- Van Gisbergen, J. A. M., Van Opstal, A. J., & Tax, A. A. M. (1987). Collicular ensemble coding of saccades based on vector summation. *Neuroscience*, *21*, 641–555.
- Van Opstal, A. J., & Van Gisbergen, J. A. M. (1989). A nonlinear model for collicular spatial interactions underlying the metrical properties of electrically elicited saccades. *Biology Cybernetics*, *60*, 171–183.
- Walker, R., Deubel, H., Schneider, W. X., & Findlay, J. M. (1997). Effect of remote distractors on saccade programming: Evidence for an extended fixation zone. *Journal of Neurophysiology*, *78*, 1108–1119.